Antal Kerpely Doctoral School of Materials Science & Technology

Surface Quality Improvement of 42CrMo4 Hard-Turned Steel by Two-Step Slide Diamond Burnishing

Claims Booklet of the Ph.D. Dissertation

By: Jawad Zaghal
(M.Sc. in Metallurgical Engineering)

Supervisor
Prof. Dr. Márton Benke
(Ph.D.)

Head of the Doctoral School
Prof. Dr. Valéria Mertinger
(D.Sc.)

Miskolc, 2024

TABLE OF CONTENTS

1. INTRODUCTION AND KNOWLEDGE GAP 1

2. THE OPEN QUESTIONS OF THE STUDY 2

3. EXPERIMENTAL SETUP 3

3.1. Material and Specimens Preparation 3

3.2. Hard-Turning, Grinding, and Polishing Conditions 3

3.3. Burnishing Conditions 3

3.4. Measuring Residual Stresses 4

3.5. Surface Roughness Measurements 5

3.6. Measuring Microhardness (HV 0.2) 5

4. RESULTS AND DISCUSSION 6

4.1. Surface Axial Residual Stress Components After the Finishing Step of SDB 6

4.1.1. Percentage of Axial Residual Stress Improvement of the Two-Step SDB Process 6

4.2. Surface Tangential Residual Stress Components After the Finishing Step of SDB 7

4.3. Relationship Between Surface Residual Stresses and Kurtosis Parameter 8

4.4. Residual Stress Depth distributions 10

4.5. Results of Surface Roughness 12

4.6. Results of Surface Microhardness 12

4.7. Results of Surface Morphology 12

4.8. Relationship Between Burnished Microstructure and In-Depth Residual Stresses Distribution 14

5. CLAIMS 16

6. PUBLICATIONS AND PRESENTATIONS 18

1. INTRODUCTION AND KNOWLEDGE GAP

The surface integrity of machined components is crucial for their functional performance, including fatigue life, wear resistance, and corrosion resistance. An optimal surface finish, which reduces potential crack initiation sites, is essential for components under cyclic loading or harsh environments. Slide diamond burnishing (SDB) improves surface quality by decreasing surface roughness, introducing compressive residual stresses, increasing microhardness, and refining the microstructure, thus enhancing overall surface integrity and fatigue life.

The initial surface roughness before burnishing significantly affects the final outcomes. Traditionally, grinding is used as a pre-burnishing process to reduce surface roughness by removing high peaks and creating a more uniform surface. However, improper grinding can introduce tensile residual stresses, leading to premature failure under cyclic loading. **Accordingly, this point has formulated the knowledge gap of this study, which shaped the literature review detailed in the next chapter.**

To mitigate the negative effects of grinding, this doctoral thesis proposes a two-step SDB process. Unlike the multi-pass SDB with consistent force, the two-step SDB varies the force between the two steps. The first step aims to reduce the initial surface roughness of hard-turned 42CrMo4 steel samples, followed by a second finishing step. Additionally, the study explores the effectiveness of SDB after polishing, which generally yields lower surface roughness than grinding.

The experimental work comprised two phases. The first phase identified optimal burnishing parameters in terms of surface roughness by burnishing 27 surfaces with various combinations of speed, feed, and force. The second phase involved hard turning, followed by different finishing processes on five bars sectioned into eight surfaces each: one bar was ground, another polished, and the remaining three were initially burnished with different forces. All surfaces then underwent a final SDB step with forces incremented by 25 N from 25 to 200 N, using optimal feed and speed settings.

Measurements of surface axial and tangential residual stresses, surface roughness (R_a), and microhardness (HV 0.2) were taken after turning, grinding, polishing, and the first burnishing step. After the finishing SDB step, these measurements were repeated, and further evaluations included in-depth residual stress distribution, 3D surface topography, surface morphology, and cross-sectional microstructure for selected surfaces.

2. THE OPEN QUESTIONS OF THE STUDY

Identifying the study's knowledge gap and conducting a literature review led to the exploration of the open question: **Is there an alternative method to reduce the initial surface roughness of the workpiece before the final SDB step, other than grinding?** To answer this, the proposed workplan illustrated in Figure 1 was developed.

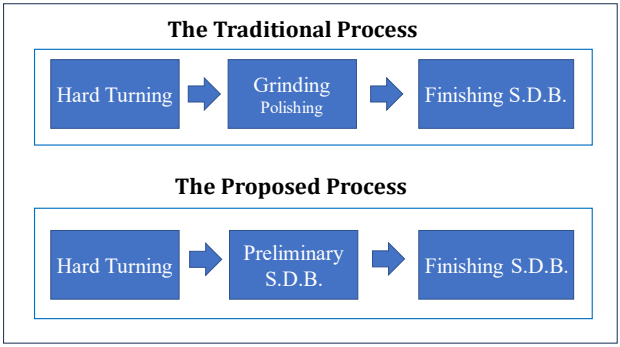

Figure 1. The proposed work plan of the Ph.D. dissertation

According to this workplan, the following open questions have been answered.

1. What are the optimal parameters (speed, feed, and force) within the examined range that result in the lowest surface roughness for steel rods subjected to hard turning during the initial SDB procedure?
2. When using the optimal burnishing speed and feed, what is the optimum burnishing force to be used in the traditional approach to achieve the best surface quality?
3. What combination of first-step and second-step burnishing forces should be used in the proposed process to achieve the highest surface quality in the finishing SDB process, characterized by low surface roughness, high compressive residual stresses, high hardness, and fine grain structure?
4. Is it possible to achieve superior surface quality (low surface roughness, high compressive residual stresses, high hardness, and improved microstructure) in hard-turned 42CrMo4 steel through a two-step SDB method compared to a single SDB process involving either grinding or polishing?
5. Is the utilization of two-step SDB instead of one-step SDB directly after turning, without subsequent process like grinding or polishing in hard-turned 42CrMo4 steel, more advantageous in terms of surface integrity components?

3. EXPERIMENTAL SETUP

3.1. Material and Specimens Preparation

The specimens were cylindrical in shape, with a diameter of 50 mm and a length of 280 mm. Each bar was partitioned into eight segments, each measuring 25 mm in length, and separated by a 5 mm gap. The overall number of bars was five. After sectioning, the workpieces underwent austenitization at a temperature of 855°C, followed by oil quenching, and then tempering for a duration of two hours at a temperature of 180°C, resulting in a hardness level of 54 HRC.

3.2. Hard-Turning, Grinding, and Polishing Conditions

Following the hardening process of the bars, the hard turning was performed on an OPTIturn S 600 CNC lathe using an insert from Mitsubishi Materials Company, model number: CNGA 120408 TA4 MB8025. The cutting speed (v_c) was set at 120 m/min, the cutting feed (f) was 0.1 mm/rev, the tool nose radius (r_ε) was 0.8 mm, and the depth of cut (a_p) was 0.2 mm.

For grinding, a CNC mantle grinder, type Studer S31, was utilized. The grinding wheel speed (v_T) was 25 m/s, the workpiece speed (n_W) was maintained at 600 rpm, the feed rate (f) was set at 700 mm/min, and the removed allowance (Z) was kept at 0.005 mm. The diameter of the corundum wheel was 400 mm, and the grain size was 80 µm. For the polishing, a manual grinder of the Bernardo DS200-400 type was utilized. The polishing speed (v_r) was set at 2850 rpm, and DIASTAR paste (diamond grit size 5.5-8 µm) was employed.

3.3. Burnishing Conditions

Samples were categorized into three groups: ground-then-burnished (G + SDB), polished-then-burnished (P + SDB), and burnished twice (two-step SDB). After grinding and polishing, each surface on every bar—which consisted of eight surfaces—was subjected to a unique burnishing force, ranging between 25 N and 200 N, in increments of 25 N between the adjacent surfaces. However, for the surfaces that underwent two-step SDB, in the first step of burnishing, the surfaces on one bar were burnished with 50 N, with 100 N on the second, and with 150 N on the third one. Subsequently, each surface on every bar was burnished in the second step with a distinct force from those ranging from 25 to 200 N.

Burnishing speed and feed remained constant across all surfaces. Based on the findings from the initial phase of this research, the combination of this speed and feed yielded the optimal results for surface roughness, as well as high axial compressive residual stresses and microhardness values. The selection of these

optimal parameters is discussed in detail in the published Q1 paper titled: **Improving Surface Integrity by Optimizing Slide Diamond Burnishing Parameters After Hard Turning of 42CrMo4 Steel** [1]. Those optimal parameters were: 0.03 mm/rev feed and 115 m/min speed.

Samples underwent burnishing using an EU-400-01 universal lathe using a burnishing tool with a 3.5 mm radius tip made of PCD (polycrystalline diamond) manufactured at the Institute of Manufacturing Science, University of Miskolc. Furthermore, burnishing was carried out using SAE 15W-40 oil.

3.4. Measuring Residual Stresses

After turning, grinding, polishing, preliminary and finishing steps of SDB, residual stress components of the two main directions were measured, namely the axial (feed) and tangential (speed) directions. The $sin^2\psi$ method was used with a Stresstech - Xstress 3000 G3R type centerless diffractometer equipped with a Cr X-ray source. For measurements, the {211} of the ferrite phase reflections were measured. During the measurements, a collimator of 2 mm in diameter was utilized. The tilting number was 5 in both tilting directions (left and right), with maximum tilting angles of $\mp 45^{\circ}$. The exposure time was chosen to be 4 seconds. Background extraction was done using linear subtraction, and the material parameters were Young's modulus of 211 GPa and Poisson's ratio of 0.3. For each surface, three measurements were taken at equal angles of 120° at the perimeter, and the average was calculated. It is worth mentioning that stress measurements were taken after the burnishing process at varying intervals—sometimes after a few days, sometimes after weeks, or even months. This variability is due to the fact that no stress relaxation occurs after burnishing; otherwise, the method would be ineffective.

After analyzing the outcomes for surface residual stresses, surface roughness, and microhardness after the finishing step of burnishing, surfaces with the optimal results were selected for further examination of their in-depth residual stresses. Besides, the in-depth residual stress distribution after turning, grinding, polishing, and the first step of burnishing was investigated. For that purpose, a QETCH 100 M electrolytic etcher from QATM was employed to remove the steel's layers, and the thickness of the etched layers was measured using the Mitutoyo ABSOLUTE depth gauge. Surface and in-depth stress measurements were carried out at the Institute of Physical Metallurgy, Metalforming and Nanotechnology at the University of Miskolc. Eventually, it is worth mentioning that for the whole measurements, the error range was less than ∓ 50 MPa.

3.5. Surface Roughness Measurements

The arithmetic mean surface roughness (R_a) of the burnished pieces was measured in the axial (feed) direction. In those measurements, the measurement length was 1.5 mm, the evaluation length was 1.25 mm, and the cut-off was 0.25 mm, chosen in accordance with ISO 21920-2:2021 for roughness measurements. Additionally, for the surfaces that underwent a two-step SDB and were burnished with 150 N in the first step, the kurtosis parameter (R_{ku}) was measured over lengths of 1.5 mm in both the axial and tangential directions. For the measurements of R_a and R_{ku}, three measurements—each of them was taken along a single line scan across the surface—were captured at equal angles of 120° around the perimeter, and the average value was calculated. In addition to the previous measurements, 3D surface topography was generated by scanning 1.5 x 1.5 mm areas for the purpose of visually assessing some selected surfaces. All of the aforementioned 2D and 3D measurements were conducted at the Institute of Manufacturing Science, University of Miskolc, using the confocal chromatic sensor on the AltiSurf 520 device.

3.6. Measuring Microhardness (HV 0.2)

After the finishing step of SDB, the microhardness of the entire surfaces was measured in the axial direction. This was conducted at the Institute of Physical Metallurgy, Metalforming and Nanotechnology at the University of Miskolc using the Wilson Instruments Tukon 2100 B device. Vickers microhardness was determined at three different points on the top of each surface using a 200-gram load, and the average value was then calculated.

4. RESULTS AND DISCUSSION

4.1. Surface Axial Residual Stress Components After the Finishing Step of SDB

The average of surface axial residual stress components after the finishing step of the SDB process are depicted in Figure 2. The dependence of the induced compressive residual stresses (CRS) magnitude on the finishing burnishing force was evident. With the five processes, a general trend was observed: An increase in the finishing burnishing force led to an increase in the generated CRS. It is seen that, using the proposed two-step SDB could give higher results than burnishing after grinding or polishing, depending on the first and second steps' forces.

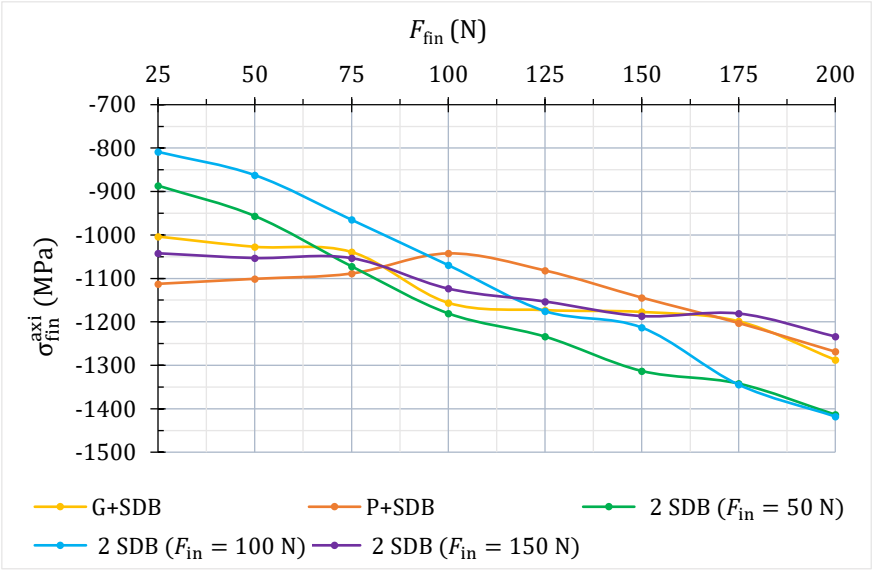

Figure 2. Surface axial residual stresses after grinding or polishing and SDB and two-step SDB processes of hard-turned 42CrMo4 steel

4.1.1. Percentage of Axial Residual Stress Improvement of the Two-Step SDB Process

A critical aspect of evaluating the two-step SDB process is assessing the improvement in axial residual stress percentage ($\%I\sigma_{axi}$). This percentage evaluates the axial stress improvement after the second step compared to the first one. Results of $\%I\sigma_{axi}$ are illustrated in Figure 3. It is critical to recognize that negative values in the outcomes represent a decrease in residual stresses from their original levels, while positive values denote an increase of these stresses.

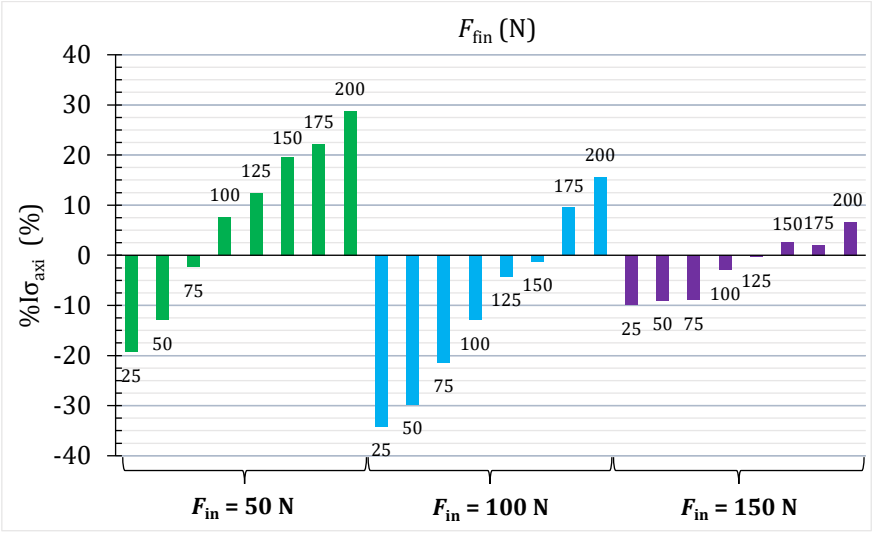

Figure 3. Improvement percentage in surface axial residual stresses for surfaces treated with two-step SDB of hard-turned 42CrMo4 steel

Assuming that the presented relationships are linear, their representing equations are listed in Table 1. Also shown in the table the second-step burnishing forces after which improvements in the axial stresses can be achieved ($F_{\text{fin}-0.0}$).

Table 1. Behavior equations of the results of the percentage of surface axial residual stress improvement after two-step SDB of hard-turned 42CrMo4 steel

F_{in} [N]	Equation	R^2 [%]	$F_{fin-0.0}$ [N]
50	$\%I\sigma_{axi} = 0.277F_{fin} - 24.2$ (9)	98	87
100	$\%I\sigma_{axi} = 0.292F_{fin} - 42.7$ (10)	99	146
150	$\%I\sigma_{axi} = 0.099F_{fin} - 13.6$ (11)	94	137

4.2. Surface Tangential Residual Stress Components After the Finishing Step of SDB

The findings of tangential stress components are illustrated in Figure 4. The predominant trend observed across all groups is a decrease in tangential stresses with higher finishing burnishing forces.

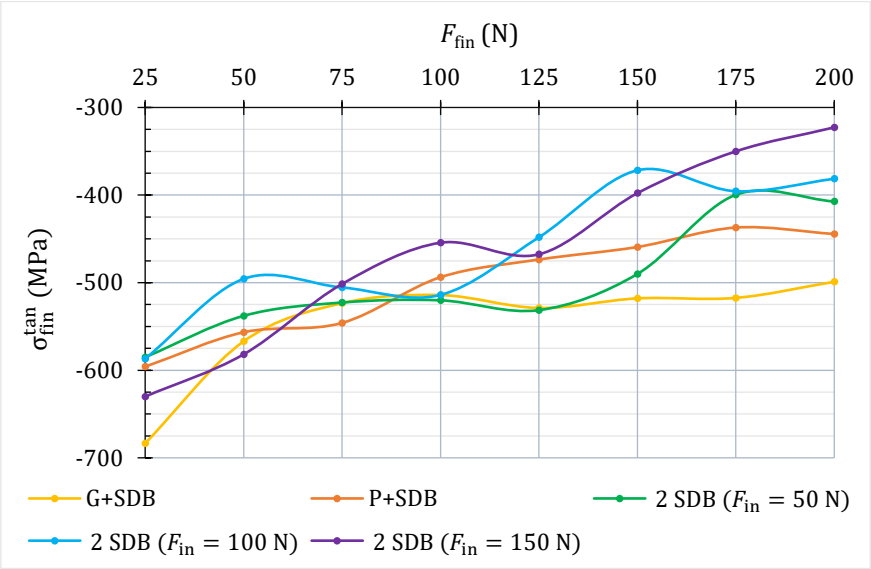

Figure 4. Surface tangential residual stresses after grinding or polishing and SDB and two-step SDB processes of hard-turned 42CrMo4 steel

Comparing the results of the traditional processes (Grinding / Polishing + SDB) with the proposed two-step SDB, it is observed that tangential stresses resulting from grinding, then burnishing, were among the highest for certain burnishing forces. Specifically, grinding, then burnishing with a 25 N force and within the 150 to 200 N range produced the highest stresses.

4.3. Relationship Between Surface Residual Stresses and Kurtosis Parameter (R_{ku})

From the results of axial and tangential surface residual stress components, it is observable that, for both one-step after grinding or polishing and two-step slide diamond burnishing processes, increasing the force in the 25-200 N range increases surface residual stresses and decreases the kurtosis coefficient (R_{ku}) (which is proportional with the sharpness of the surface profile) in the axial direction (Figure 5), however, it decreases surface residual stresses and increases R_{ku} in the tangential direction (Figure 6).

The cause is attributed to the relative velocity between the workpiece surface and burnishing head, which is 1916 mm/s in the tangential direction, compared to 0.03 mm per revolution in the axial direction. The high tangential velocity, combined with an increase in burnishing force, led to increased sharpness with numerous

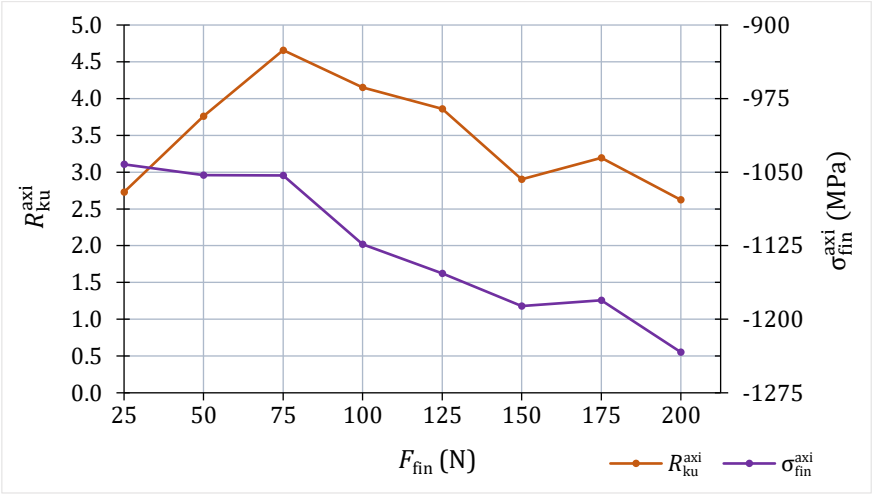

Figure 5. Relationship between surface residual stresses and average kurtosis coefficient ($\boldsymbol{R_{ku}}$) in the axial direction of surfaces after two-step SDB burnished by 150 N in the first step of hard-turned 42CrMo4 steel

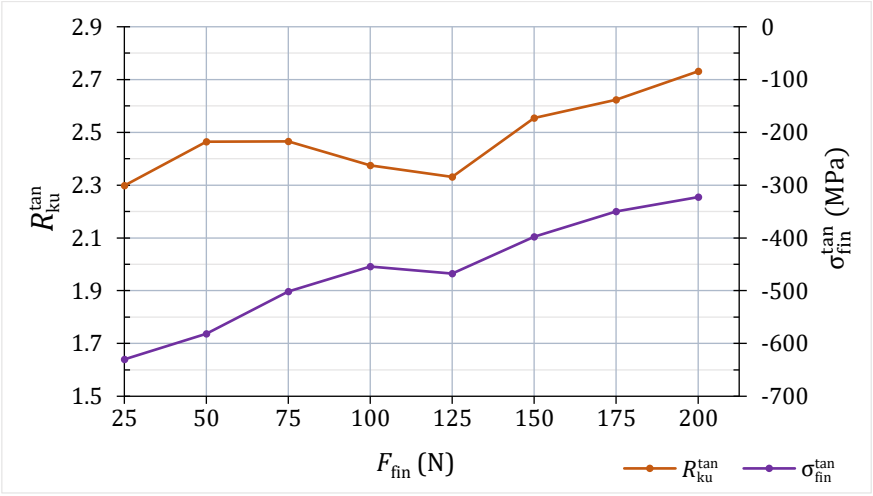

Figure 6. Relationship between surface residual stresses and the average kurtosis coefficient ($\boldsymbol{R_{ku}}$) in the tangential direction of surfaces after two-step SDB burnished by 150 N in the first step of hard-turned 42CrMo4 steel

narrow peaks that deflect easily and retain minimal residual stresses. With a further increase in burnishing force, the sharpness increased, leading to greater stress relaxation. This effect was more pronounced on surfaces treated with the two-step

slide diamond burnishing process compared to those treated with the traditional one. This is attributed to the diminution in toughness that occurred after the first burnishing step, particularly on the surfaces burnished with forces of 100 and 150 N in the first step. When these surfaces were subsequently burnished with forces larger than 100 N, the impact of this phenomenon increased significantly compared to the traditional process due to surface fatigue caused by applying high forces to the brittle surfaces.

On the other hand, in the axial direction, the very low velocity resulted in lower sharpness with wider peaks, which resist bending and retain large residual stresses. The effect of this phenomenon in getting larger axial stresses was significantly greater with surfaces burnished by 50 and 100 N in the first step, followed by forces larger than 100 N in the second step, compared to those treated with the traditional process. The reason behind that is the brittleness induced into those surfaces after the first step of burnishing. Consequently, in the second step, less burnishing energy is consumed by friction for further smoothing the surface via slip deformation along slip planes. Instead, more energy is available to induce additional compressive residual stresses.

4.4. Residual Stress Depth distributions

When comparing the results of the in-depth residual stress distribution of the surfaces burnished using the two-step SDB process, it was found that burnishing with 150 N in the first step and with 200 N in the second step achieved the best results among the three groups of surfaces.

Compared to slide diamond burnishing with 200 N after grinding or polishing, two-step slide diamond burnishing performed with 150 N and then 200 N achieves greater axial and tangential compressive residual stresses in depth, as depicted in Figure 7. Moreover, compared to one-step slide diamond burnishing performed with 200 N after turning, this surface results in larger axial residual stresses from the depth of 0 to ~200 μm and larger in-depth tangential residual stresses from 10 μm to ~220 μm as shown in Figure 8.

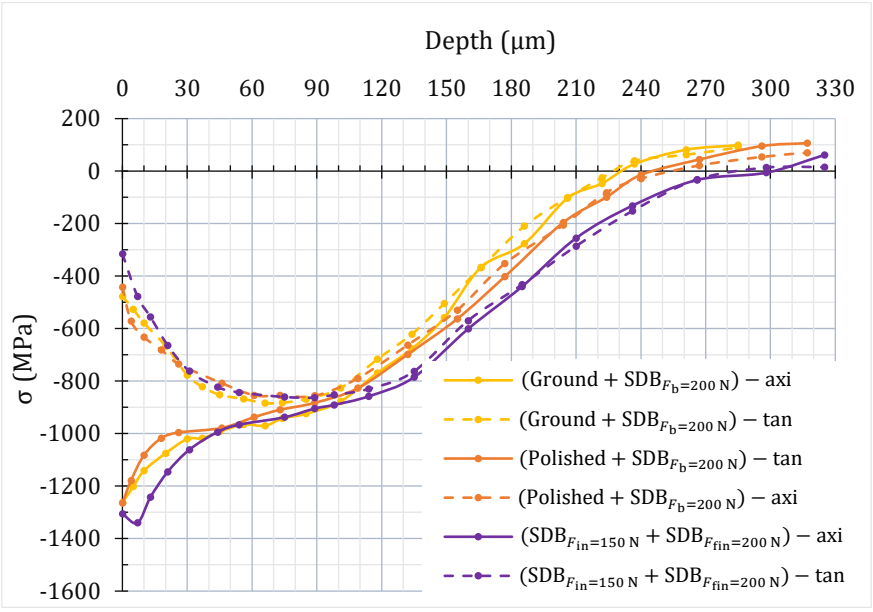

Figure 7. In-depth residual stress distribution of hard-turned 42CrMo4 steel after grinding and SDB, polishing and SDB, and two-step SDB using 150 N and then 200 N forces

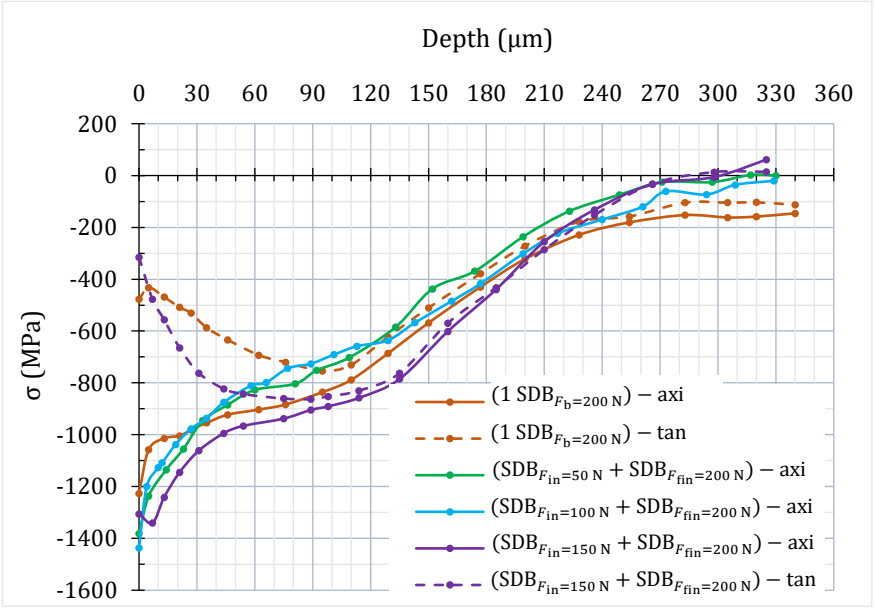

Figure 8. In-depth residual stress distribution after one-step and two-step SDB methods of hard-turned 42CrMo4 steel

4.5. Results of Surface Roughness

Concerning the results of R_a surface roughness, it could be seen from Figure 9 that two-step slide diamond burnishing performed with 150 N and then 200 N achieves lower R_a surface roughness compared to slide diamond burnishing with 200 N after grinding or polishing. Additionally, when comparing with 0.068 µm roughness achieved by one-step SDB performed after turning, this surface burnished by two-step SDB was smoother.

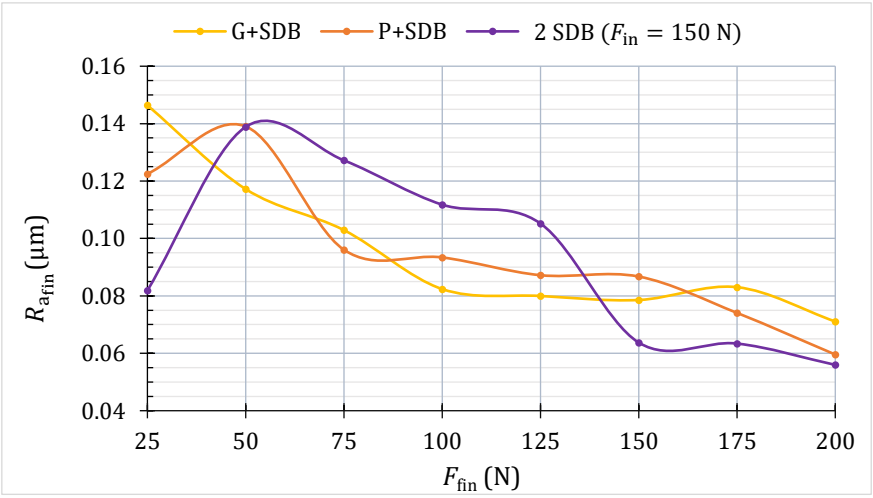

Figure 9. Surface roughness of hard-turned 42CrMo4 steel after grinding and SDB, polishing and SDB, and two-step SDB using 150 N and then 200 N forces

4.6. Results of Surface Microhardness

When it comes to the results of surface microhardness (HV 0.2), according to the results shown in Figure 10, two-step slide diamond burnishing performed with 150 N and then 200 N achieves greater surface microhardness compared to slide diamond burnishing with 200 N after grinding or polishing. Additionally, when comparing with 752 HV 0.2 microhardness achieved by one-step SDB performed after turning, this surface burnished by two-step SDB was harder.

4.7. Results of Surface Morphology

Figure 11 (a) depicts the morphology of the surface treated with grinding and SDB. It can be seen that despite the is characterized with parallel lines or striations that run across the surface and are perpendicular to the axial feed direction. Additionally, wave-like patterns or ripples are present, likely caused by the lateral flow of material during the burnishing process.

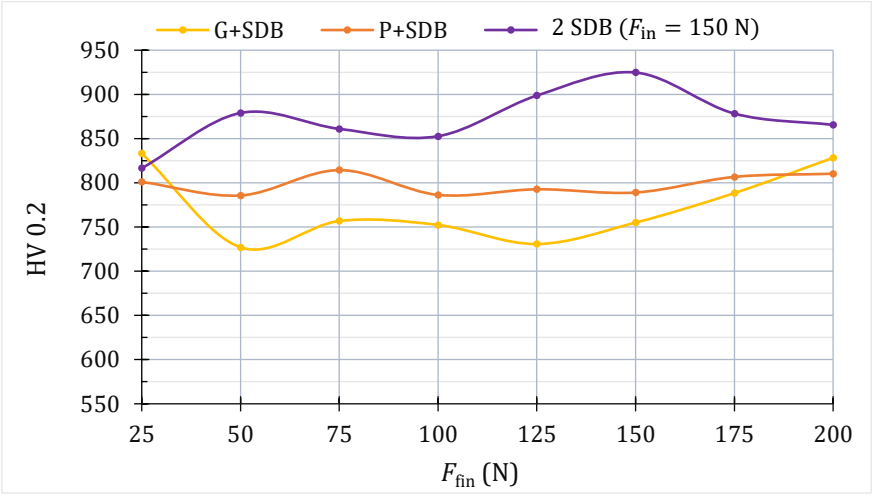

Figure 10. Surface microhardness of hard-turned 42CrMo4 steel after grinding and SDB, polishing and SDB, and two-step SDB using 150 N then 200 N forces

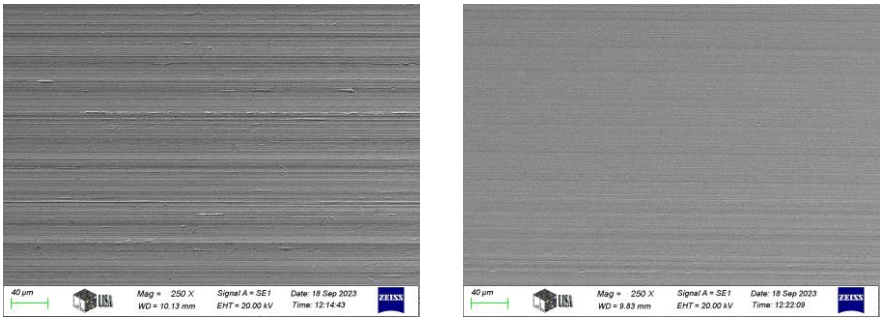

(a) Grinding + $SDB_{F_b=200N}$ (b) $SDB_{F_{in}=150N}$ + $SDB_{F_{fin}=200N}$

Figure 11. SEM images of surface morphology of hard-turned 42CrMo4 steel after grinding and SDB, polishing and SDB, and two-step SDB using 150 N and then 200 N forces

Moreover, a remarkable characteristic of this surface is the presence of feed marks generated by the burnishing head due to the high force applied during the burnishing process, which are noticeable despite the steel's hardened state. Alongside these, various defects and imperfections, such as pits, scratches, protrusions, and microcracks, are detected.

On the other hand, Figure 11 (b) shows the surface morphology of the material that has undergone a two-step SDB process, with the first step executed using 150 N following the turning process and the second step performed by 200 N. The surface

exhibits a high degree of uniformity and smoothness, with an improved finish. In addition, the morphology of the surface is characterized by highly refined linear striations, indicative of a substantial initial flattening of surface irregularities.

4.8. Relationship Between Burnished Microstructure and In-Depth Residual Stresses Distribution

When it comes to the zone below the visible plastic deformation—which extends from the surface to a depth less than 10 μm, it is proposed that plastic deformation (slip) also occurs in this region in the tangential direction. This can be explained by the variation of tangential and axial stress components until they reach a depth where they gain similar value, as depicted in Figure 12.

In the plastic deformation zone of grains—which extends from the surface to the peak of the tangential stresses—there is slip in the tangential direction. Near the surface, the slip is notable due to the high shear strain rate, causing the visible plastic deformation of grains and, consequently, an intensive decrease of elastic lattice distortion in the tangential direction. Moving further in depth, the occurrence of slip decreases, and the elastic distortion increases. Slip remains present until the depth where the tangential and axial stress components equalize. This depth marks the end of the plastic deformation zone.

However, in the axial direction, no slip occurs near the surface due to the low shear strain rate. As a result, the elastic distortion of the lattice is not reduced. Upon moving further in depth, the elastic distortion continuously decreases. The in-depth residual stress distribution shown at the bottom of Figure 12 illustrates this interaction between the two stress components. Finally, at the end of the plastic deformation zone, no slip occurs, and the tangential and axial stress components equalize. Beyond this point, both stress components continue to decrease at the same rate until reaching the end of the elastic deformation zone.

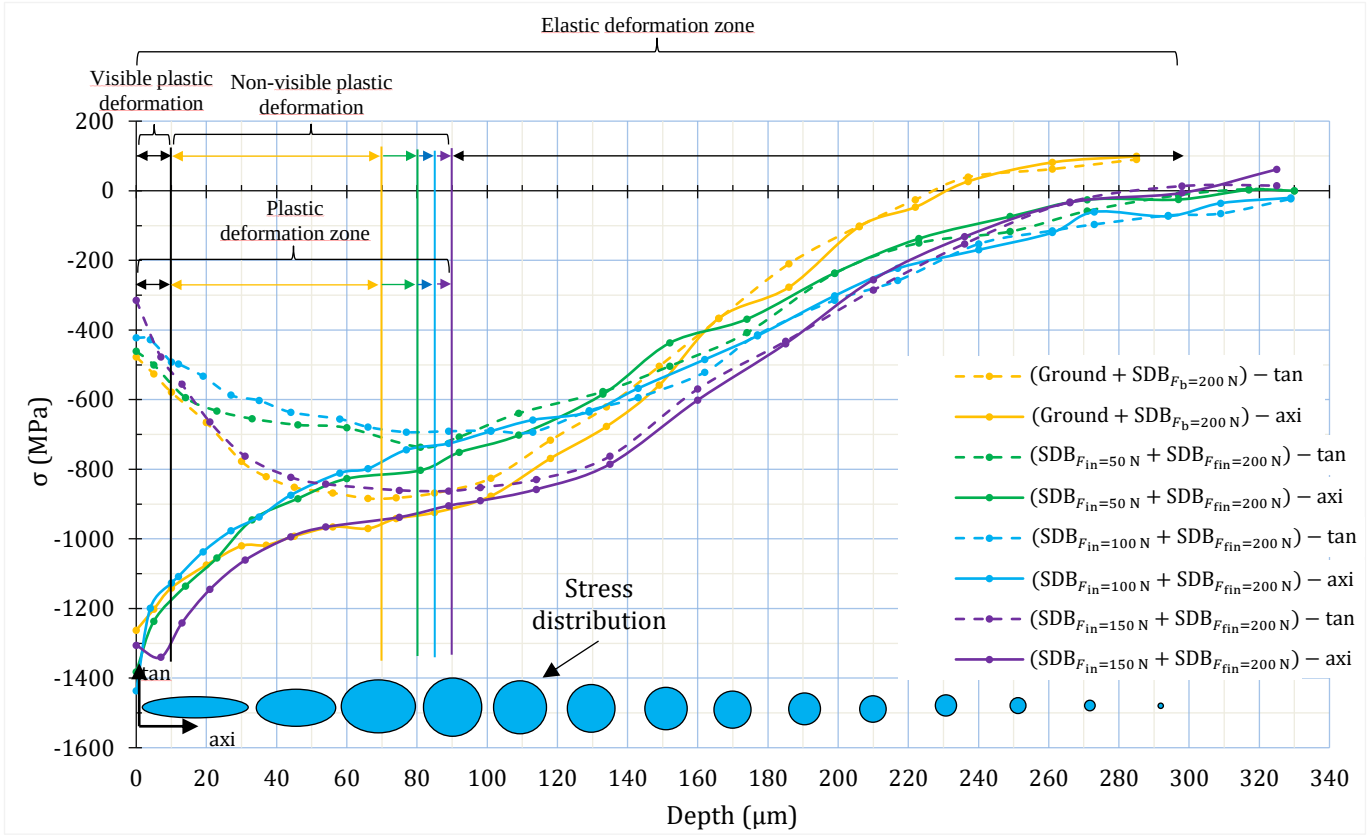

Figure 12 In-depth components of axial and tangential residual stresses and their respective zones after one and two-step SDB

5. CLAIMS

The following claims are valid for hard-turned 42CrMo4 steel with a hardness of 54 HRC and slide diamond burnishing using the optimum parameters of the examined values: a feed of 0.03 mm/rev and a speed of 115 m/min.

- Claim No. 1:

The proposed two-step slide diamond burnishing process performed with 150 N and then 200 N achieves the same level of compressive axial stress component on the surface, larger compressive axial and tangential stress components in depth, lower R_a surface roughness, higher HV 0.2 microhardness, and a flawless surface compared to single-step slide diamond burnishing with 200 N after grinding or polishing. The reason is that, in the second step of burnishing, less energy is consumed by friction compared to single-step slide diamond burnishing.

- Claim No. 2:

For the proposed two-step slide diamond burnishing process, increasing the second-step burnishing force in the 25–200 N range increases surface residual stresses and decreases the kurtosis parameter (R_{ku}) in the axial direction; however, it decreases surface residual stresses and increases R_{ku} in the tangential direction. The cause is attributed to the relative velocity between the workpiece surface and burnishing head, which is 1916 mm/s in the tangential direction and 0.03 mm per revolution in the axial direction. Under these very different velocities, the shear strain rates are completely different, and the material deforms differently. The high tangential velocity combined with an increase in burnishing force leads to increasing sharpness with more, narrow peaks, which deflect easily and retain minimal residual stresses. On the other hand, the low axial velocity combined with an increase in burnishing force leads to decreasing sharpness with less, wider peaks, which resist deflection and retain large residual stresses.

- Claim No. 3:

In the proposed two-step slide diamond burnishing process, axial surface residual stresses can be further improved in the second step compared to the first one when burnishing in the second step is done with at least ~87 N, ~146 N, and ~137 N when the first step is done with 50 N, 100 N, and 150 N, respectively.

- Claim No. 4:

The proposed two-step slide diamond burnishing process performed with 150 N and then 200 N results in larger compressive axial stress components from the depth of 0 to ~200 μm, larger in-depth compressive tangential stress components from ~10 μm to ~220 μm, lower R_a surface roughness, and higher HV 0.2 microhardness compared to one-step slide diamond burnishing performed with 200 N. Moreover, two-step slide diamond burnishing performed with 50 N or 100 N and then 200 N achieves larger compressive axial stress components from the depth of 0 to ~30 μm compared to one-step slide diamond burnishing performed with 200 N. The reason is that, in the second step of burnishing, less energy is consumed by friction compared to single-step slide diamond burnishing.

- Claim No. 5:

In two-step slide diamond burnishing and burnishing after grinding, in the tangential direction, plastic deformation of grains (slip) does not only happen in the visible plastic deformation zone but until the tangential and axial stress components become almost equal. High shear strain rates near the surface in the tangential direction cause significant slip, leading to visible plastic deformation and reduced elastic lattice distortion. As depth increases, slip decreases, and the elastic distortion of the lattice increases, causing an increase in tangential stresses. Upon reaching the end of the plastic deformation zone, slip finishes and the elastic lattice distortion equalizes for the tangential direction and axial direction, in which no slip occurs due to low shear strain rates.

6. PUBLICATIONS AND PRESENTATIONS

1. **Local Conference Presentation:** "Characterization of Residual Stresses Induced into Bearing Rings by Means of Turning in Soft State Using Different Turning Parameters", *New Results in Materials Science*. Miskolc, 2021.

2. **J. Zaghal**, V. Mertinger, A. Filep, G. Varga, and M. Benke, "Characterization of residual stresses induced into bearing rings by means of soft turning using different turning parameters," *J. Mach. Eng.*, vol. 21, no. 4, pp. 49–56, 2021, **Independent Citations: 1**, 10.36897/jme/144299

3. **J. Zaghal**, V. Mertinger, Á. Filep, and M. Benke, "Characterization of residual stress state after turning of bearing rings". *Doktorandusz Almanach*, vol. 1, pp. 313-318, 2022, **Independent Citations: 1**, http://epa.niif.hu/04600/04692/00001/pdf/EPA04692_doktorandusz_almanach_2022_313-318.pdf

4. **J. Zaghal**, V. Molnár, and M. Benke, "Improving surface integrity by optimizing slide diamond burnishing parameters after hard turning of 42CrMo4 steel," *Int. J. Adv. Manuf. Technol.*, pp. 1–17, 2023, **Independent Citations: 2**, 10.1007/s00170-023-12008-6

5. **J. Zaghal** and M. Benke, "Determination of reliable area sizes for 3D roughness measurement," *Cut. & Tools Technol. Syst.*, no. 98, pp. 3–12, 2023, **Independent Citations: 1**, https://doi.org/10.20998/2078-7405.2023.98.01